CLM-P782

CLM-P782

UKAEA

Preprint

SPURIOUS BEHAVIOUR OF NUMERICALLY COMPUTED FLUID FLOW

J. W. EASTWOOD
W. ARTER

CULHAM LABORATORY
Abingdon, Oxfordshire
1986

CLM-P 782

SPURIOUS BEHAVIOUR OF NUMERICALLY COMPUTED FLUID FLOW

James W Eastwood and Wayne Arter

Culham Laboratory, Abingdon, Oxfordshire, OX14 3DB, UK

(Euratom/UKAEA Fusion Association)

Abstract

We investigate the stability to aliasing errors of numerical schemes for hydrodynamics, taking the viscous Burgers' equation as a model for systems with a term quadratic in the velocity. Considering wavelengths equal to three times the mesh-spacing and arbitrary mean flow, we are able to demonstrate explicitly for common schemes (a) a sufficient criterion for stability and (b) blow-up of solutions in a finite time when (a) is violated. For these schemes, singular behaviour is shown to persist at all wavelengths: studies of wavelengths up to thirty times mesh-spacing make it clear that a profile with a single region of strong convergent flow is most conducive to instability. In contrast, spectral (Galerkin) and upwind schemes are shown to be stable for all flows and periods.

(Submitted for publication in IMA Journal of Numerical Analysis)

June 1986

1. Introduction

It has long been recognised that aliasing errors can cause blow-up of numerically computed solutions of in particular the 2-D vorticity equation (Phillips, 1959). The precise mechanism is best understood by thinking in terms of the Fourier transformed fluid equations and variables. Suppose the shortest wavelength that can be represented on the necessarily discrete computational mesh has wavenumber k_c. If the velocity spectrum is filled for k up to k_c, then the nonlinear advection term attempts to generate flows with wavenumbers up to $2k_c$. Those in the range $k_c + 1$ to $2k_c$ are aliased, ie misidentified with flows of wavenumber less than k_c (eg Hockney and Eastwood, 1981, Chap 5). Energy which should have been transferred to short wavelengths reappears instead at long wavelengths. When the physical process being modelled is a cascade of energy to small scales, clearly a feedback instability is possible. Our study is motivated by the need to understand simulations of experiments that may exhibit sudden, violent behaviour, eg disruptions in tokamaks (Eastwood and Arter, 1986a). Under these circumstances it may be difficult to distinguish physical from numerical effects. This paper is part of an attempt to understand what happens when the latter predominate.

Finite difference as well as pseudospectral calculations are prone to instability caused by aliasing error which may operate even when linear stability criteria such as Courant-Friedrichs-Lewy are satisfied. One way around the problem has been to design finite difference schemes which conserve quadratic invariants such as the total energy in a flow (Arakawa, 1966). These, loosely speaking, turn out to be an example of Galerkin methods (fully spectral schemes are another) which in general lead to bounded results

(Morton, 1977, pp731-740). However, other finite difference schemes remain popular, and pseudospectral methods (which allow aliasing and are not generically energy conserving) are more efficient than fully spectral ones (Orszag and Israeli, 1974).

Thus an as general as possible study of aliasing instability seems desirable, and we choose Burgers' equation as the simplest model of fluid dynamics capable of exhibiting the effect. (It is apparent that our results should also apply to incompressible flows.) Fornberg (1973) has already shown there is a growing short wavelength solution for the inviscid case, unless difference schemes of Arakawa type are employed. We shall include the viscous term, and in addition ensure that our solutions satisfy linear stability criteria by looking at the limit of schemes when timestep $\Delta t \to 0$ (the semi-discrete limit). D.F.Griffiths (private communication) has carried out a wide-ranging study of the inviscid Burgers' equation on similar lines. For a recent work discussing nonlinear stability criteria in the semi-discrete limit for the Burgers' equation see Griffiths (1982, after eg Pen-Yu and Sanz- Serna, 1981) - again the construction of nonincreasing energy-like quantities is crucial.

Here we consider the time-dependent behaviour of solutions of Burgers' equation which have a wavelength equal to N mesh-points, ie the flow $u(x)$ is represented by $\{u_j\}$, where $j = 0,1,\ldots,N$ is the label corresponding to position x. A systematic treatment of $N > 3$ is hard, because as $\Delta t \to 0$ the numerical schemes reduce to a system of nonlinear ordinary differential equations, with an N-dimensional phase space spanned by the u_j. Sanz-Serna (1985) has discussed the stability of

leapfrog schemes for the inviscid Burgers' equation using a semi-discrete method that entails considering a 2Nth order system.

Section 2 shows that is possible to establish stability at general N for spectral and upwinding schemes, where by stability we shall mean that as $\Delta t \to 0$, each u_j can be shown to remain bounded for all time. Section 3 considers a variety of other schemes for N=3 only, which all turn out to exhibit instability. Section 4 specialises to one of these conditionally unstable schemes and looks at the effect of increasing N to 4 and 5. In an independent investigation, Aref and Daripa (1984) have briefly considered N = 3 and 4 for this scheme. Section 5 advances to the limit of large N. Lastly, Section 6 provides a summary and a discussion.

2. General Results.

Burgers' equation (Bateman, 1915; Burgers, 1948) models the 1-D time-dependent flow $u(x,t)$ of compressible fluid with viscosity ν :

$$\frac{\partial u}{\partial t} + u \frac{\partial u}{\partial x} = \nu \frac{\partial^2 u}{\partial x^2} \quad . \tag{1a}$$

The equation is made dimensionless by scaling u by ν/L and t by t_d, where $t_d = L^2/\nu$ is the diffusive time-scale and L is a naturally occurring length-scale. This gives

$$\frac{\partial u}{\partial t} + u \frac{\partial u}{\partial x} = \frac{\partial^2 u}{\partial x^2} \quad . \tag{1b}$$

It is instructive to multiply (1b) by u^{n-1} and integrate over a distance equal to the wavelength of u (assumed periodic) giving

$$\frac{\partial}{\partial t}\int u^n dx = -(n-1)\int \left(\frac{\partial u}{\partial x}\right)^2 u^{n-2}\,dx \qquad (2)$$

We see that the mean flow $\bar{u}$ is conserved, and the square integral of u decays until $u = \bar{u}$.

However, the nonlinearity of (1b) may be removed using the Cole-Hopf transformation $u = -2\,\partial(\ln\theta)/\partial x$. For the particular initial conditions $u = -R\sin x$, this gives the subsequent time development

$$u(x,t) = \frac{2\sum_{n=1}^{\infty} n a_n \exp(-n^2 t)\sin(nx)}{\sum_{n=0}^{\infty} a_n \exp(-n^2 t)\cos(nx)}, \qquad (3)$$

where $a_n(R) = c_n I_n([R/2])$ with $c_0 = 1$, $c_n = 2(-1)^n$ otherwise, and I_n is the exponentially increasing Bessel function of the second kind. Note that the initial conditions imply $u(2\pi) = u(0)$ - this helps to keep (3) simple, elsewhere in the paper we have imposed $u(1) = u(0)$. R plays the role of Reynolds number, so it follows that when $R \gg 1$, for times shorter than the diffusive time-scale, steep gradients of u develop in regions of converging flow (Cole, 1951; Lighthill, 1956, Section 10.4). It is there that aliasing errors arise. Note that (3) is non-singular because the initial u maps to a positive definite θ: such a θ remains positive for finite times (and its gradient $\partial\theta/\partial x$ also decreases).

To compute solutions to (1) we introduce a representation for u in terms of a finite set of values $\{u_j\}$, $j = 0,\ldots,N-1$ and usually advance $\{u_j\}$ explicitly in time with a step limited by $\Delta t \leq \max(\alpha_1 h/u_m,$

$\alpha_2 h^2/\nu)$ where u_m is the maximum $|u_i|$, h is the mesh spacing and α_1 and α_2 are O(1) constants depending on the numerical scheme. Taking the limit $\Delta t \to 0$ gives a set of equations

$$\dot{u}_j = N_j(u_0,\ldots u_{N-1}) + L_j(u_0,\ldots u_{N-1}), \quad j = 0,\ldots,N-1 \qquad (4)$$

where $(N_j)L_j$ is a (non-)linear operator. Note that we do not move into the reference frame where $\bar{u} = 0$ because the operators N_j and L_j may not be invariant under this transformation.

For the spectral method, $\{u_j\}$ are the finite Fourier transform (FFT) of the real function u and thus are complex numbers with $u_j^* = u_{N-j}$, where the star denotes complex conjugate. We use the conventions for normalising FFTs given by Hockney and Eastwood (1981, Appendix). It is then convenient to make (1a) dimensionless by scaling time with respect to $(Nh)^2/(4\pi^2\nu)$ and u_j with respect to $2\pi\nu$. We find

$$\frac{d}{dt}\sum |u_j|^2 = \sum (N_j u_j^* + N_j^* u_j) - 2\sum j^2 |u_j|^2, \qquad (5)$$

where

$$N_j = (-i) \sum_{0 \leq j-j' \leq N-1} j' u_{j'} u_{j-j'}, \qquad (6)$$

and the other sums are over 0 to N-1. The first term of (5) may be written, apart from a multiplicative factor, as

$$\sum\sum_{0 \leq j-j' \leq N-1} \left(j' u_j, u_{j-j'}, u_{N-j} - j' u_{N-j'}, u_{j'}, {}_{-j} u_j\right) \quad . \tag{7}$$

Exchanging labels of the second term gives

$$\sum\sum (j' - j)\, u_j, u_{j-j'}, u_{N-j} \tag{8}$$

$$= - \sum\sum j' u_j, u_{j-j'}, u_{N-j} \tag{9}$$

where we have written j' for $j-j'$. If we set $T = \sum N_j u_j^*$, (9) shows $T + T^* = -T$, ie $T = 0$. The second term of (5) leads to decay of all u_j , $j \neq 0$.

Next we show the upwind schemes yield bounded, decaying solutions. Here, and for the other finite difference schemes (unless otherwise stated) we rescale u by ν/h , time by h^2/ν and set

$$L_j = \left(u_{j+1} - 2u_j + u_{j-1}\right) \quad . \tag{10}$$

If all $u_j > 0$, then upwinding gives

$$N_j = - u_j(u_j - u_{j-1}) \quad . \tag{11}$$

We see

$$\frac{d}{dt} \sum u_j = -\sum u_j^2 + \sum u_j u_{j-1} = R_j \quad . \tag{12}$$

Maximising the right hand side with respect to u_j gives at each j,

$$u_{j-1} - 2u_j + u_{j+1} = 0 \quad , \tag{13}$$

or u_j = constant. $R_j < 0$ otherwise, hence $\sum u_j$ decays until u_j = constant. If some of the u_j are negative, we consider d/dt $\sum (|u_j|)$ to derive an expression analogous to (12) which contains $-\sum u_j^2$ and other terms all of the form $u_j u_{j-1}$. The argument proving stability goes through as above unless there is duplication among the latter terms. This only occurs when u_j and u_{j-1} are of opposite sign (in fact $u_{j-1} < 0$ and $u_j > 0$), ie such terms are negative and therefore can only cause $\sum |u_j|$ to decrease. The L_j terms further contribute to the reduction, until eventually all the u_j have the same sign.

Another upwinding scheme sets $N_j = -(u_j^2 - u_{j-1}^2)/2$ when all $u_j > 0$. It follows that, provided the u_j have the same sign, $\sum u_j$ is conserved, thereby ensuring solutions remain bounded. If the u_j change sign, there is no conservation law and the reader is directed to Engquist and Osher (1980) for a proof of stability for general N. The case N=3 is further discussed in Section 3.3.

3. Period Three Results

3.1 Pseudospectral Method

The pseudospectral method requires two representations of u. Let $\{u_j\}$, $j = 0,1,2$ be the values of u at equally spaced points $x = x_j$ and introduce the finite Fourier transform for dimensionless variables

$$\tilde{u}_j = \sum' u_{j'} \exp(-i2\pi jj'/N) \quad . \tag{14}$$

The model equations may be developed as for the spectral method with $\tilde{u}_j$ taking the role of u_j, but the nonlinear term (6) is formed without restricting $k = j-j'$ to $\{0,1,\ldots,N-1\}$, identifying wavenumbers $k < 0$ or $k > N-1$ with $k' = mN + k$ where the integer m is chosen so that $0 \leq k' \leq N-1$. Note that this prevents the relabelling of (8) to give (9), and hence solutions can no longer be proved to stay bounded. Adopting the units of the spectral problem, (4) becomes

$$\dot{\tilde{u}}_0 = 0 \quad , \tag{15a}$$

$$\dot{\tilde{u}}_1 = i\left(-\tilde{u}_1^2 + \tilde{u}_0\tilde{u}_1\right) - \tilde{u}_1 \quad . \tag{15b}$$

Writing $\tilde{u}_0 = c$ $(= u_0 + u_1 + u_2 = 3\bar{u}$ where $\bar{u}$ is the conserved mean flow), then setting $\tilde{u}_1 = x + iy = re^{i\theta}$ gives the equations

$$\dot{x} = -2xy - cy - x \quad , \tag{16a}$$

$$\dot{y} = -x^2 + cx + y^2 - y \quad , \tag{16b}$$

or equivalently

$$\dot{r} = -r(r\sin 3\theta + 1) \quad , \tag{17a}$$

$$\dot{\theta} = c - r\cos 3\theta \quad . \tag{17b}$$

Note the threefold symmetry caused by the invariance of the problem under cyclic relabelling of the points and the presence of fixed points with $r = (1 + c^2)^{\frac{1}{2}}$, $\sin 3\theta = -1/r$.

A set of equations such as (16) cannot in general be solved analytically, and although when $c = \nu = 0$, $\mathrm{Im}(u_1) = y$ may be found as function of x since (16) is then homogeneous of degree 2, it is more revealing to produce a phase-plane portrait (figure 1). This is made easier when a simple (r, θ) representation such as (17) is available. (17a) shows at once that $\dot{r} \leq 0$ when $r < 1$, equality being achieved only at the origin. $r = 0$ corresponds to the uniform equilibrium $u =$ constant, to which the pseudo-spectral method has thus been shown to asymptote, provided $r < 1$. If $c = 0$, there is a fixed point when $r = 1$, $\theta = \pi/2$, which is unstable. For $r(0) > 1$, setting $c = 0$, $\theta = \pi/2$ enables us to construct solutions which become infinite in a finite time. (17) becomes $\dot{r} = r^2 - r$, $\dot{\theta} = 0$, which may be trivially integrated to give

$$(1 - r)^{-1} + (r(0) - 1)^{-1} = e^{-t} \quad . \tag{18}$$

Writing $\rho = (r(0) - 1)^{-1} > 0$ if $r(0) > 1$, yields

$$r = 1 + \left(\rho - e^{-t}\right)^{-1} \quad , \tag{19}$$

which becomes infinite at a time $t = O(1)$.

These results become easier to understand if we return to dimensional u_j-space variables. We use Parseval's theorem for a finite Fourier

transform $v_j \to \tilde{v}_j$,

$$\sum |\tilde{v}_j|^2 = h^2 N \sum v_j^2 \quad , \tag{20}$$

with $v_j = u_{dj} - \bar{u}_d$, to show

$$v_{rms} = \left(\frac{1}{N} \sum v_j^2\right)^{1/2} = \frac{2\pi\nu 2^{1/2} r}{hN} \quad . \tag{21}$$

Suffix d denotes a dimensioned quantity. Note the factor of $\sqrt{2}$ resulting from the Hermitian symmetry of the FFT. We see that $r < 1$ corresponds to

$$Re_m = \frac{h\, v_{rms}}{\nu} < \frac{2^{3/2}\pi}{3} \simeq 2.96 \quad , \tag{22}$$

where Re_m is the root-mean-square mesh Reynolds number. The line $\theta = \pi/2$ corresponds to $\{u_j\}$ antisymmetric, ie $u_0 = 0$, $u_1 = -u_2$ (coinciding with the $\{u_j\}$ studied by Fornberg (1973)) and blow-up occurs on the mesh diffusion time-scale $t_{dm} = h^2/\nu$. Contrast this behaviour with that of the analytic solution (3).

The role of nonzero (without loss of generality positive) mean flow is not quite as simple as (17) at first suggests. Although $r < 1$ obviously remains a sufficient condition for stability for all $c > 0$, it is possible that the critical Re_m increases with c since the unstable fixed point moves out to a radius $r_c = (1 + c^2)^{1/2}$.

Numerically computing the solutions of (16) suggests that in the limit of large c, the domain of attraction of the origin approaches the triangle which has the unstable fixed points as vertices, see Figure 2.

This is confirmed by introducing co-ordinates $\xi = (3^{1/2}x - y)/2$, $\eta = (x + 3^{1/2}y)/2$, and considering a triangle T which has the above properties, viz that with vertices $(x,y) = (r_c,0)$, $(-r_c/2, \pm 3^{1/2}r_c/2)$. The side lying in $0 < \theta < 2\pi/3$ is mapped to $\eta = r_c/2$: elementary manipulation shows that on this line $\dot{\eta} = (c - r_c)\xi - r_c/2$. The greatest value of $\dot{\eta}$ is $\dot{\eta}_{max} = r_c(3^{1/2}[r_c - c] - 1)/2$ at the vertex $\xi = -3^{1/2}r_c/2$ and more algebra shows $\dot{\eta}_{max} < 0$ provided $c > 3^{-1/2}$. By symmetry, the phase space flow is everywhere into T. The inscribed circle of T has radius $r = r_c/2$, thus we have shown the critical $r \propto c/2$ for $c >> 1$. If we introduce the mesh Reynolds number for the mean flow $\overline{Re} = h\bar{u}_d/\nu$, we find $\overline{Re} = 2\pi c/3$ and thus the critical $Re_m \to 2^{-1/2}\overline{Re}$. The most unstable flow has two equal u_i.

3.2 Finite Difference Methods

We consider schemes with a conservative and a non-conservative representation of the non-linear term, respectively setting

$$N_j = (u_{j-1}^2 - u_{j+1}^2) \quad , \tag{23}$$

$$N_j = u_j(u_{j-1} - u_{j+1}) \quad , \tag{24}$$

where to yield these N_j we have non-dimensionalised u_j with respect to

the factor $4\nu/h$ (23) and $2\nu/h$ (24). Thus, eg.(24) yields a set of equations

$$\begin{aligned}
\dot{u}_0 &= u_0(u_2 - u_1) + (u_1 - 2u_0 + u_2) \quad , \\
\dot{u}_1 &= u_1(u_0 - u_2) + (u_2 - 2u_1 + u_0) \quad , \\
\dot{u}_2 &= u_2(u_1 - u_0) + (u_0 - 2u_2 + u_1) \quad .
\end{aligned} \tag{25}$$

Analysis of (25) and its analogues is helped by introducing variables $\{\tilde{v}_j\}$, the finite Fourier transform of $v_j = u_j - \bar{u}$. Since both (23) and (24) conserve $\sum u_j$ [(23) also has $\sum u_j^3$ as an invariant when $\nu = 0$] the dimension of the system is reduced by one in symmetric fashion, and the diffusion operator is also simplified. Writing $\tilde{v}_1 = re^{i\theta}$, the conservative scheme gives

$$\begin{aligned}
\dot{r} &= -3^{-1/2} r\,(r\sin 3\theta + 3^{3/2}) \quad , \\
\dot{\theta} &= -3^{-1/2}\,(r\cos 3\theta + 2c) \quad ,
\end{aligned} \tag{26}$$

whereas (25) becomes,

$$\begin{aligned}
\dot{r} &= 3^{-1/2} r\,(r\sin 3\theta - 3^{3/2}) \quad , \\
\dot{\theta} &= 3^{-1/2}\,(r\cos 3\theta - c) \quad .
\end{aligned} \tag{27}$$

(26) and (27) may be brought into the form of (17) by rescaling t by a factor of 3, r by $3^{-3/2}$, redefining c, and for (27) additionally

making the transformation $\theta \to -\theta$. Using Parseval's theorem as in Section 3.1 shows that (26) and (27) have critical Re_m of $4\sqrt{6} \approx 9.80$ and $2\sqrt{6} \approx 4.90$ respectively, when $c = 0$. In the limit of large c , the critical $Re_m = 2^{1/2}\,\overline{Re}$ for the conservative scheme and $= 2^{-1/2}\,\overline{Re}$ for the non-conservative one. The properties of the $\{u_j\}$ that are the likeliest to blow up are the same as for the pseudospectral method.

3.3 A Second Upwinding Scheme

This upwinding scheme, discussed briefly in Section 2, is known to be stable for all N. If when N=3 one of the u_j has a different sign to the others, say $u_0<0$, u_1, $u_2\geq 0$, it leads to the dimensionless equations

$$\begin{aligned}
\dot{u}_0 &= u_0^2 - u_1^2 + u_2 - 2u_0 + u_1, \\
\dot{u}_1 &= u_0^2 - u_1^2 + u_0 - 2u_1 + u_2, \\
\dot{u}_2 &= u_1^2 - u_2^2 + u_1 - 2u_2 + u_0.
\end{aligned} \tag{28}$$

However, it seems (28) can still be misleading, for unlike the other schemes studied, when $\nu=0$ it possesses stable fixed points with u of differing signs. This follows by studying small amplitude perturbations about the point $2u_i=(-a,a,a),a>0$: if a time dependence $\alpha\, e^{St}$ is assumed, S satisfies

$$S(S+a)(S+2a)=0. \qquad (29)$$

The root $S=0$ corresponds to translations along the line L in phase space generated as a varies, the others are negative, implying L is attracting. For $\nu\neq 0$, (28) possesses no equilibria with $u_0<0$, $u_1,u_2>0$, but solutions still rapidly approach the neighbourhood of L when ν is small, and we discover that soon $2u_j \simeq (-b,b,b)$ where $\dot{b} = O(-\nu)$. Thus if (28) is integrated numerically for times short compared to the diffusion time it appears that solutions reach an equilibrium on L. Only at much later times is a solution with equal u_j reached, and $\sum u_j$ may have meanwhile been reduced by orders of magnitude. Taking $Re_m < O(1)$ will diminish these spurious effects.

4. Nonconservative Difference Scheme

4.1 Period 4 Results

If a solution of the Burgers' equation is initially antisymmetric about some point, it remains so. Similarly, antisymmetry is preserved by the discrete equations. Aref and Daripa (1984) have used this property to reduce (24) with $N=4$ to a 2nd order system. (Note that antisymmetry implies zero mean flow, $\bar{u} = 0$.) The phase space plot that results is similar to Figure 1, but containing only two (because of the projection) unstable fixed points $u_0 = -u_3 = (1 + \sqrt{2})$, $u_1 = -u_2 = (-1 + \sqrt{2})$.

It is natural to enquire whether the distance Re_{mp} from the origin of the closest unstable fixed point does indeed give the critical Re for stability when $c=0$, and what is the c-dependence of Re_{mp}. The

solution of the nonlinear fixed point equations for general c is aided by use of MACSYMA (Bogen et al, 1983). It transpires that there is a unique set of fixed points, given parametrically as

$$(u_0, u_1, u_2, u_3) = (S, -(\frac{S+1}{S-1}), -\frac{1}{S}, \frac{S-1}{S+1}), \tag{30}$$

where S is related to c by

$$c = (S^4 - 6S^2 + 1)/[S(S^2 - 1)]. \tag{31}$$

Re_m for the points given by (30) satisfies

$$Re_m^2 = \frac{4}{N} \sum (u_j - \bar{u})^2 = \frac{3\ (1 + S^2)^4}{4S^2(S^2 - 1)^2}. \tag{32}$$

Eliminating S between (31) and (32) we see $Re_{mp}^2 = 12 + 3c^2/4$. Thus the least Re_{mp} occurs when $c = 0$, $S^2 = (1 \pm \sqrt{2})^2$. Direct substitution shows that such S correspond to antisymmetric $\{u_j\}$.

The fixed points are unstable for any c. We linearise the period 4 equations about the point (30). If solutions varying as $\exp(\sigma t)$ are sought, straightforward manipulation gives

$$\sigma(\sigma^3 + 8\sigma^2 + \beta(S)\sigma + \gamma(S)) = 0. \tag{33}$$

It is at once evident that (30) is always unstable, since

$$\gamma(S) = - \frac{4(S^2 + 1)^4}{S^2(S^2 - 1)^2} , \qquad (34)$$

and the Routh-Hurwitz criterion requires $\gamma > 0$.

There is one significant contrast with the results for N=3 with c=0; stability is no longer guaranteed for points with $Re_m \leq Re_{mp}$. To see this it suffices to determine the separatrices at the unstable fixed points in the antisymmetric system. This enables us to sketch the phase space behaviour near eg the point (30) given by $S = 1 + \sqrt{2}$. Figure 3 makes it clear how flows with $Re_m \leq Re_{mp}$ may be attracted to the fixed point and thereafter expelled towards infinity (see also below).

To determine a bound on Re_m which guarantees stability, we must transform the u_j rather like we did in Sections 3.1 and 3.2. First we introduce the co-ordinates suggested by inspection of the four-point Fourier transform, viz.

$$c = u_0 + u_1 + u_2 + u_3 ,$$

$$x = u_0 - u_2 ,$$

$$y = u_1 - u_3 ,$$

$$z = u_0 - u_1 + u_2 - u_3 .$$

(35)

This reduces the order of system to be studied to three. Next we introduce spherical polars (r, θ, ϕ) so that r is proportional to Re_m, ie,

$$(x, y, z) = [r/2](\cos\theta\sin\phi, \cos\theta\cos\phi, \sin\theta/\sqrt{2}) \qquad (36)$$

We find r satisfies

$$\dot{r} = -r(1 + \sin^2\theta) - 2\sqrt{2}\, r^2(\sin\theta - \sin^3\theta)\sin 2\phi . \qquad (37)$$

The r^2 term in (37) is most destabilising when $\sin 2\phi = \pm 1$ corresponding to antisymmetric $\{u_j\}$. Setting $\dot{r} = 0$, we have

$$r = \frac{(1 + \sin^2\theta)}{\sqrt{2}\sin\theta(1 - \sin^2\theta)} , \qquad (38)$$

which is least when $\sin\theta = \pm\sqrt{(\sqrt{5} - 2)}$, $r = (\sqrt{5} - 1)/[\sqrt{2}(3 - \sqrt{5})\sqrt{\{\sqrt{5} - 2\}}]$. This r provides a bound Re_{mr} (independent of c) upon Re_m which ensures that solutions have non-increasing kinetic energy. $Re_{mr} \approx 3.330\,191$ is only 4% smaller than $Re_{mp} = \sqrt{12} \approx 3.46$, so Re_{mp} is still a good estimate for the critical Re_m, which satisfies $Re_{mr} < Re_m < Re_{mp}$.

The asymptotic behaviour of the divergent solutions is obtained by neglecting the linear (diffusive) terms in the governing ODEs, and seeking solutions

$$u_j = \beta_j/(t_0 - t), \; j = 0, \; 1, \; 2, \; 3. \tag{39}$$

Straightforward manipulation shows that $\beta_j = (1, -1, 0, 0)$ and cyclic permutations thereof are the sole solutions of form (39) for N = 4. We go on to show these solutions are attracting in the large u_j (inviscid) limit.

Suppose we have two trajectories, differing slightly in starting point, one initially at β_j/t_0 on the singular trajectory and the other described by $[\beta_j + \varepsilon_j(t)]/(t_0 - t)$. At time t, the difference in rate of travel along the two trajectories (labelled 1 and 2) is given by

$$(\dot{u}_1 - \dot{u}_2)_j = \frac{d}{dt}\left(\frac{\varepsilon_j}{t_0 - t}\right)$$

$$= \alpha_{jk\ell}\frac{(\beta_k + \varepsilon_k)(\beta_\ell + \varepsilon_\ell) - \beta_k\beta_\ell}{2(t_0 - t)^2}, \tag{40}$$

where we have introduced $\alpha_{jk\ell}$ such that $\dot{u}_j = \frac{1}{2}\alpha_{jk\ell}u_k u_\ell$ (using the summation convention). Since $\alpha_{jk\ell}$ is symmetric in its last two indices, (40) yields

$$(t_0 - t)\dot{\varepsilon}_j = (\alpha_{jk\ell}\beta_\ell - \delta_{jk})\varepsilon_k \; . \tag{41}$$

Assuming that there exist co-ordinates such that $\alpha_{jk\ell}\beta_\ell = \lambda_{(j)}\delta_{jk}$, (41) has solutions $\alpha(t_0 - t)^{1-\lambda_j}$. Thus the trajectories 1 and 2 converge provided $\lambda_j < 1$ for each eigenvector perpendicular to the singular one. There is always one $\lambda_j = 2$, corresponding to differential motion parallel to (39). For the N = 4 Burgers' equation, $\lambda_j = (-1, -1, 0, 2)$, hence the asymptotic solution of form (39) is attracting.

4.2 Period 5 Results

We now repeat the analysis of the previous section for the 5th order problem. The fixed points are calculated parametrically as

$$
\begin{aligned}
u_0 &= S, \\
u_1 &= \frac{-[S^2 + 3(1 + \sqrt{5})S + \sqrt{5}]}{S^2 + (-3 + \sqrt{5})S + 2 + \sqrt{5}}, \\
u_2 &= \frac{(2 + \sqrt{5})S^2 - 2(2 + \sqrt{5})S - \sqrt{5}}{S^2 + 2\sqrt{5}\,S + 1}, \\
u_3 &= -\frac{\left[(2 + \sqrt{5})S^2 + 2(3 + \sqrt{5})S + \sqrt{5}\right]}{S^2 - 4\,S - 1}, \\
u_4 &= \frac{S^2 + (-7 + \sqrt{5})S - \sqrt{5}}{S^2 + (-1 + \sqrt{5})S - 2 + \sqrt{5}}.
\end{aligned}
\qquad (42)
$$

The relation between c and S is not very revealing, nor is the analogue of equation (32). However, we are again able to eliminate S, yielding $Re_{mp}^2 = 80 - 32\sqrt{5} + 16c^2/25$. Thus the least Re_{mp} is again when c = 0, for which it follows that S = 0, and the u_j are antisymmetric. Sketching the

phase space for N = 5, assuming antisymmetric $\{u_j\}$ (Figure 4) shows that the fixed points are again unstable, and solutions started in their neighbourhood may diverge to infinity.

To estimate the critical Re_m, we introduce the co-ordinates suggested by the five-point Fourier transform, viz,

$$c = u_0 + u_1 + u_2 + u_3 + u_4 ,$$

$$x_1 = u_0 + (2\gamma^2 - 1)(u_1 + u_4) - \gamma(u_2 + u_3) ,$$

$$x_2 = u_0 - \gamma(u_1 + u_4) + (2\gamma^2 - 1)(u_2 + u_3) , \qquad (43)$$

$$y_1 = 2\sigma\gamma(u_1 - u_4) + \sigma(u_2 - u_3) ,$$

$$y_2 = \sigma(u_1 - u_4) - 2\sigma\gamma(u_2 - u_3) .$$

Here $\gamma = \cos(\pi/5)$, $\sigma = \sin(\pi/5)$, so that $\sigma^2 + \gamma^2 = 1$ and $4\gamma^2 - 2\gamma - 1 = 0$. Next we convert to hyperspherical co-ordinates (r, θ, ϕ, ψ) given by:

$$(x_1, x_2, y_1, y_2) = 5r(2\sigma)^{-1}(\cos\theta\sin\phi, \sin\theta\sin\psi, \cos\theta\cos\phi, \sin\theta\cos\psi). \qquad (44)$$

Setting $\delta = 2\gamma$, we find r satisfies

$$\dot{r} = -r\left[2 + \delta + (1-2\delta)\cos^2\theta\right] + \left[r^2/2\right]\sin 2\theta \; x$$
$$\left[(1 - 2\delta)\cos\theta\cos(2\phi-\psi) + (2+\delta)\sin\theta\cos(2\psi+\phi)\right]. \qquad (45)$$

The most unstable r occurs when $\cos(2\phi-\psi) = 1$, $\cos(2\psi+\phi) = \pm\cos(2\phi-\psi)$. It is not immediately apparent as how the sign should be taken. Moreover, if we equate $\dot{r}$ to zero and seek to minimise r over $\cos\theta$, we find the extremal $\cos\theta$ satisfy a quintic equation. Thus it is more efficient to proceed numerically, plotting (45) as a function of θ for $\cos(2\psi+\phi) = \pm 1$. By inspection $\cos(2\psi+\phi) = 1$ gives the least r for which $\dot{r} = 0$. Such values of ψ and ϕ correspond to antisymmetric $\{u_j\}$. The corresponding θ satisfies $\cos\theta \simeq 0.801$, yielding $Re_{mr} \simeq 2.77$. This is to be compared with $Re_{mp} \simeq 2.91$: thus we have determined the critical Re_m to within 5%, since it must lie between Re_{mr} and Re_{mp}.

We finish the section by showing that there are attracting solutions which asymptotically diverge as $(t_0 - t)^{-1}$, just as for $N = 4$. There are now two families of solutions, with $\beta_j = (1, -1, 0, 0, 0)$ and $\beta_j = (2, -1, 1, -2, 0)$. (General solutions may be constructed for any N and also for the pseudo-spectral scheme.) Performing the stability analysis, the addition of another zero component to the first β_j simply results in an extra $\lambda_j = 0$, hence the corresponding solution remains stable. For the new family, however, we find $\lambda_j = (-1, 0, 0, 2, 3)$, thus it is not attracting. Ultimately all solutions must join the first family.

5. Nonconservative Difference Scheme - Longer Periods

It becomes increasingly difficult to establish rigorous results as N increases, because of the complexity of the algebra. Although using MACSYMA it is possible to establish some exact results for $10 > N > 5$, we do not reproduce them. Moreover, the partial results that are available serve only to bear out the pattern established with $N \leq 5$. They cannot address the problem of great interest, viz. what happens for $N \geq 0(10)$, i.e. for periods equal to the mesh-sizes that might be used in typical, realistic simulations. Progress can be made numerically, but at the expense of making this section more heuristic than the others.

The problem of finding the fixed points of the Nth order system can be formulated as the minimisation of $\sum_{j=0}^{N-1} \dot{u}_j^2$ subject to the constraint that $\sum_{j=o}^{N-1} u_j = c$. (The analytic expression for the $\{u_j\}$ given by Crocco (1965) diverges when periodic boundary conditions are imposed.) The optimisation problem is carried out numerically with the aid of the NAG routine E04UAF, which employs a quasi-Newton method. The principal difficulty is the tendency for the trivial solution $u_j = c/N$ to be found: in part this can be prevented by setting the variable STEPMX $\geq 10^5$. For $N \leq 5$ the results obtained analytically were reproduced as a test to an accuracy of 5 decimal places. At these N, the choice of starting point, provided it is distant from $\underset{\sim}{u} = \underset{\sim}{0}$, is not critical. However, as N is increased it is necessary to commence with a good estimate of the final solution. There is evidence from the residuals that the accuracy is little changed at high N.

The values of NRe^2_{mp} for the fixed points when $c = 0$ are tabulated in Table I. These are all achieved for antisymmetric solutions of full period: with the normalisation employed here, the period 3 fixed point has $NRe^2_{mp} = 144$ if used to construct a period 6 point, compared to 40 for the point of full period. There is also evidence that NRe^2_{mp} increases $\propto c^2$ at each N, just as for $N \leq 5$.

The problem of determining Re_{mr} may be formulated as a constrained minimisation of $\Sigma u_j \dot{u}_j$ similar to that for Re_{mp}, and indeed the remarks on the numerics made above also apply here. The sole difference is that the calculation of Re_{mr} does not depend on c, for consider

$$\sum u_j \dot{u}_j = \sum u_j^2(u_{j-1} - u_{j+1}) + \sum(u_j u_{j+1} - 2u_j^2 + u_j u_{j-1}) \qquad (46)$$

Writing $u_j = w_j + \bar{u}$, $\sum w_j = 0$, we find

$$\frac{d}{dt} \sum(w_j^2 - u_j^2) = \bar{u}^2 \sum(u_{j-1} - u_{j+1}) - 2\bar{u}\sum u_j(u_{j-1} - u_{j+1})$$

$$- \bar{u} \sum(u_{j+1} - 2u_j + u_{j-1}) , \qquad (47)$$

and all the sums on the right hand side vanish because the u_j are periodic. Hence it suffices to calculate Re_{mr} with $c = N\bar{u} = 0$, and these are listed in Table I. As expected $Re_m = Re_{mr}$ occurs for antisymmetric $\{u_j\}$, and except for $N = 3$, Re_{mr} is always slightly (less than about 10%) smaller than Re_{mp}. $NRe^2_{mr} \to 35.00$ as N increases.

Further insight is obtained by plotting the u_j corresponding to the critical point closest to the origin as a function of j at Re_{mp} and Re_{mr} for the largest N computed (Figure 5). We compare with the limit $h \to 0$, $Nh = 1$ of the difference equations for these $\{u_j\}$, viz, Burgers' equation in the case of Re_{mp}. For Re_{mr} (N finite),

$$u_j + \lambda\left(1 + \left[u_{j+1} - u_{j-1}\right]/2\right)\left(u_{j+1} + u_{j-1} - 2u_j\right) = 0, \quad j=0,\ldots, N-1, \quad (48)$$

where

$$\lambda = \frac{\sum u_j^2}{\sum u_j(u_{j+1} - u_j)}. \quad (49)$$

Writing $u(x)$ for $\{u_j\}$, $x = jh$, where h is the mesh-spacing, and taking the differential limit gives $\lambda = -\lambda_o h^{-2}$, where $\lambda_o = 2\int u^2 dx / \int u'^2 dx$, and hence (48) becomes

$$u - \lambda_o\left(1 + hu'/2\right)u'' = 0, \quad (50)$$

prime denoting differentiation with respect to x.

Unless u' is very large, (50) has solutions $\propto \exp(\lambda_o^{-1/2}x)$. Replotting Figure 5b on a log-log scale (Figure 5c) shows that apart from where u is nearly discontinuous, it is indeed exponential with the theoretically predicted coefficient. Similarly Figure 5a shows that $\{u_j\}$ for Re_{mp} is approximating the exact steady state $u = 2\pi\tan\pi(x - x_o)$ of the Burgers' equation. This implies that the increase of NRe_{mp}^2 with N

will not become significant, because for N even (there is a similar expression for odd N), it implies we have as $N \to \infty$,

$$NRe_{mp}^2 \sim \sum_{j=o}^{N-1} 4\frac{\pi^2}{N^2} \tan^2 \frac{\pi(j + \frac{1}{2})}{N} = 4\pi^2\left(1 - \frac{1}{N}\right) \qquad (51)$$

The right-hand-side of (51) has the value 38.16 for $N = 30$ and thereafter it changes very little, $NRe_{mp}^2 \to 39.48$ as $N \to \infty$. The correspondence between the analytic and numerical results implies that we have in each case exhausted the likely forms for the extremal $\{u_j\}$ as $N \to \infty$. Further the c^2 dependence of Re_{mp}^2 also follows, as Figure 5d makes plain: a solution $u = 2\pi\tan\pi(x - x_o)$ is again approached, but a mesh-point m lies closer to x_o so that $u_m \simeq c$. Assuming that the limiting function is always the tangent, it is not apparent that the constraint $\sum u_j = c$ can be more economically met. Lastly, it becomes reasonable that there should be solutions in the vicinity of the $\{u_j\}$ plotted in Figure 5 that ultimately exhibit $(t_o - t)^{-1}$ behaviour, remembering that at any N there is an attracting asymptotic solution of sharply discontinuous form

$$u_j = (0, \ldots, 0, 1, -1, 0, \ldots, 0)/(t_o - t). \qquad (52)$$

Hence Re_{mr} and Re_{mp} bound the critical Re_m in the large N limit also.

6. Summary and Discussion

We can classify numerical schemes for the Burgers' equation in terms of their nonlinear stability in the limit $\Delta t \to 0$. The schemes divide

into two classes: those which may be shown to be stable for any mesh size and flow, and others for which solutions become unbounded if the Reynolds number is too large - equivalent to the existence of a critical viscosity - (Sadourny, 1975). For the conditionally stable schemes we have shown solutions may become infinite in a finite time of order the mesh diffusion time-scale t_{dm}, if the critical Reynolds number is exceeded.

As to the norm in which to measure the critical Reynolds number, attention has been focussed on the root-mean-square, since this relates simply to the total kinetic energy in a calculation, and we have used the mesh-spacing h as scale-length. The scaling of the critical Reynolds number so defined, $Re_m \propto N^{-1/2}$ as the period N increases, implies that the maximum total energy scales as N in the limit with $Nh=1$. For non-zero mean flow $\bar{u} \neq 0$, stability is improved; although the energy may initially (unphysically) increase, the bound is now set in order of magnitude solely by the existence of a second, unstable solution to Burgers' equation. In this case the maximum energy scales as N^2. Kellogg et al (1980) and Stephens and Shubin (1981) have derived bounds ensuring uniqueness of steady solutions of the conservative formulation of Burgers' equation for general N and $\bar{u} = 0$; however, the case $\bar{u} = 0$ is exactly when uniqueness and stability need not be equivalent, as demonstrated in Sections 4 and 5 for a nonconservative scheme.

We believe that the schemes studied should exhibit similar properties when applied to the equations of incompressible hydrodynamics. It is reasonable that, at large N, the most unstable flow profile should again be one with a single region of strong convergence. Just how strong this needs to be is suggested by the Burgers' equation result: the unstable

$\overline{u} = 0$ velocity profile swings by 4 units in one mesh-interval. Taking into account the normalisation employed, this gives $t_u < 8t_{dm}$ for stability, where t_u is the local turnover time, defined as the inverse velocity derivative and t_{dm} is the mesh diffusion time. For the unstable schemes with $N = 3$, variations in the critical Re_m are apparently due to damping arising from the discretion of the spatial derivative - the pseudospectral scheme, for which this is least, has the severest criterion. This relation between the schemes' critical Re_m may therefore also hold very generally; further, it should be reflected in the coefficient appearing in the stability criterion $t_u < O(t_{dm})$. There is some uncertainty, in view of Phillips' discovery (1959) of an exponentially diverging solution, as to whether $(t_o - t)^{-1}$ blow-up does occur for the conditionally stable schemes applied to incompressible flows. The addition of a dynamically active magnetic field can, however, lead to this super-exponential kind of failure (Arter and Eastwood, 1986; Eastwood and Arter, 1986a).

The spectral scheme is stable for all mesh sizes and (periodic) flows because like all members of the class of Galerkin schemes, it has in the inviscid limit a positive definite quadratic invariant (Morton, 1977). Stability of upwinding is achieved at the expense of considerable damping, which leads in particular to the non-conservation of total momentum (if non-zero). Of the stable schemes we recommend EPIC (Eastwood and Arter, 1986b), which gives optimally accurate results for both periodic and more general flows.

We caution however that we are discussing stability only in the limit of vanishing Δt. When the time integration is discretised, the quantity

conserved for a simple explicit scheme is $\sum u_j^{(n)} u_j^{(n+1)}$ where (n) denotes time level, thus nonlinear instability is not excluded (Kreiss and Oliger, 1972; Sadourny, 1975; Sanz-Serna, 1985). For long wavelengths, Briggs et al (1983) have also discovered a focussing instability (although their work was in the inviscid limit). Such instabilities, concerned more with the temporal than the spatial discretisation, are outside the scope of the present paper, although the focussing instability may well be related to our discovery that the critical energy for instability decreases with increasing wavelength.

Acknowledgements

We thank Dr. L.N. Trefethen for a helpful discussion, and a referee for pointing out the closed form for the series sum in equation (51).

Table I

(a) NRe^2_{mp} (a measure of the norm of the most dangerous unstable fixed point) and (b) NRe^2_{mr} (bound ensuring solutions have non-increasing kinetic energy) tabulated as functions of N, the number of mesh-points per period.

N	(a) NRe^2_{mp} (c = 0)	(b) NRe^2_{mr}
3	72	72
4	48	44.36
5	42.23	38.32
6	40	36.29
7	38.96	35.52
8	38.43	35.20
9	38.15	35.08
10	38.01	35.03
12	37.91	35.00
15	37.95	35.00
17	38.02	35.00
20	38.13	35.00
25	38.30	35.00
30	38.44	35.00

References

A Arakawa, "Computational design for long-term numerical integration of the equations of fluid motion: two-dimensional incompressible flow. Part 1", J Computational Phys 1 (1966) pp119-143

H Aref and P K Daripa, "Note on finite difference approximations to Burgers' equation", SIAM J Sci Stat Comput 5(1984), pp856-864

W Arter and J W Eastwood, "The effect of aliasing error upon numerical solutions of the hydrodynamic and magnetohydrodynamic equations", to appear in Transport Theory and Statistical Phys (1986)

H Bateman, "Some recent researches on the motion of fluids", Mon Weather Rev 43 (1915) pp163-170

R Bogen et al, MACSYMA Reference Manual, Mathlab Group, MIT(1983)

W L Briggs, A C Newell and T Sarie, "Focusing: a mechanism for instability of nonlinear finite difference equations", J Computational Phys 51 (1983), pp83-106

J M Burgers, "A mathematical model illustrating the theory of turbulence", Advances in Appl Mech 1, Academic Press, New York, 1948, pp171-199

J D Cole, "On a quasi-linear parabolic equation occurring in aerodynamics", Quart Appl Math 9 (1951) pp225-236

L Crocco, "A suggestion for the numerical solution of the steady Navier-Stokes equations", AIAA J 3 (1965), pp1824-1832

J W Eastwood and W Arter, "An interpretation of disruptions in tokamak simulations", submitted to Phys Rev Lett (1986a)

J W Eastwood and W Arter, "EPIC - beyond the ultimate difference scheme", in Numerical Methods for Fluid Dynamics II (K W Morton and M J Baines eds), OUP (1986b), pp581-594

B Engquist and S Osher, "Stable and entropy satisfying approximations for transonic flow calculations", Math Computation 34 (1980) pp45-75

B Fornberg, "On the instability of leap-frog and Crank-Nicolson approximations of a nonlinear partial differential equation", Math Computation 27 (1973) pp45-57

D F Griffiths, "The stability of finite difference approximations to nonlinear partial differential equations", Instit Math Applic 18 (1982) pp210-215

R W Hockney and J W Eastwood, "Computer simulation using particles", McGraw-Hill, New York, 1981

R B Kellogg, G R Shubin and A B Stephens, "Uniqueness and the cell Reynolds number", SIAM J Numer Anal 17 (1980), pp733-739

H Kreiss and J Oliger, "Comparison of accurate methods for the integration of hyperbolic equations", Tellus 24 (1972) pp199-215

M J Lighthill, "Viscosity effects in sound waves of finite amplitude", Surveys in Mechanics, G K Batchelor and R M Davies eds, Cambridge University Press, Cambridge, 1956, pp250-351

K W Morton, "Initial-value problems by finite difference and other methods", The State of the Art in Numerical Analysis, D A H Jacobs ed, Academic Press, London, 1977, pp699-756

S A Orszag and M Israeli, "Numerical simulation of viscous incompressible flows", Ann Rev Fluid Mech 6 (1974), pp281-318

K Pen-Yu and J M Sanz-Serna, "Convergence of methods to the numerical solution of the Kortweg-de Vries equation", IMA J Num Anal 1 (1981) pp215-221

N A Phillips, "An example of non-linear computational instability", The Atmosphere and the Sea in Motion, B Bolin ed, Rockefeller Institute Press, New York (1959) pp501-504

R Sadourny, "The dynamics of finite-difference models of the shallow-water equations", J Atmos Sci 32 (1975), pp680-689

J M Sanz-Serna, "Studies in numerical nonlinear instability I: Why do leapfrog schemes go unstable?", SIAM J Scientific Stat Computing 6 (1985), pp923-938

A B Stephens and G R Shubin, "Multiple solutions and bifurcation of finite difference approximations to some steady problems of fluid dynamics", SIAM J Sci Stat Comput 2 (1981), pp404-415

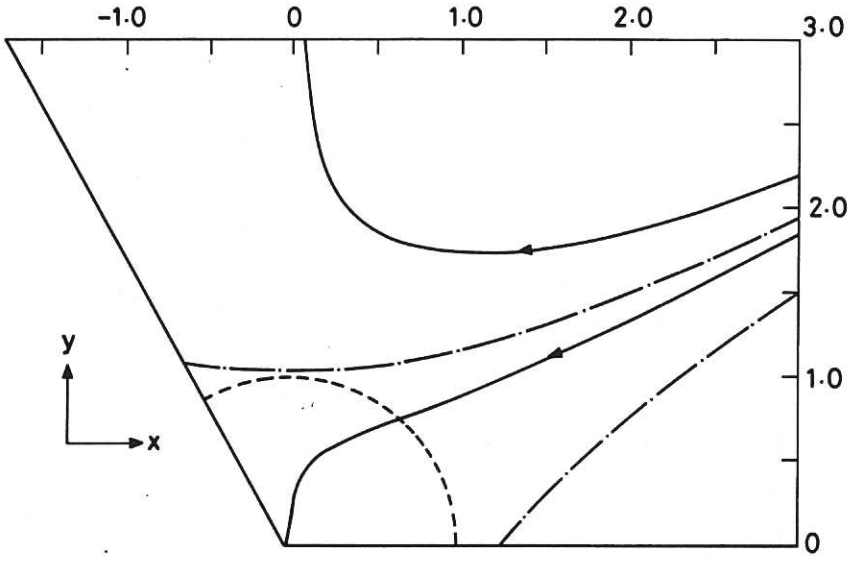

Fig. 1 Phase-planed portrait of the system (16) when $c=0$, for $0 < \theta < 2\pi/3$ (remainder of plane follows by symmetry). The dashed line is $r=1$. Note that for $r > 1$ some solutions go off to infinity, while others enter the region of attraction of the origin; the boundary between the two regions is drawn with a chained line.

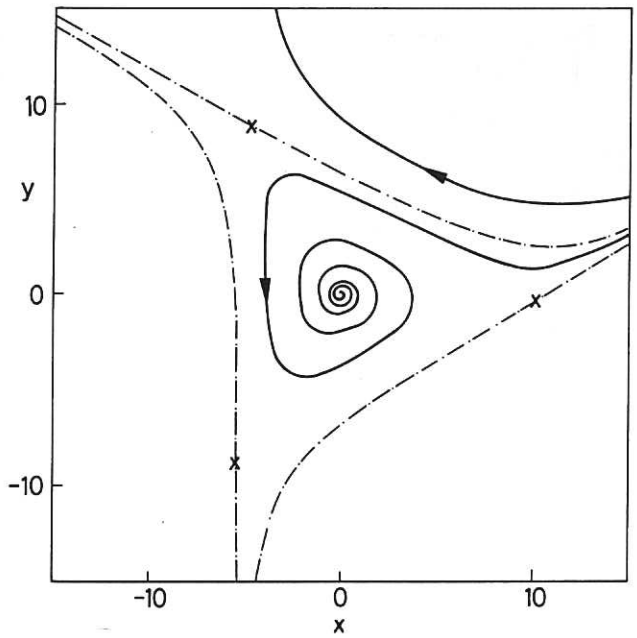

Fig. 2 Phase-plane portrait of the system (16) when $c=10$. Crosses mark the fixed point. The chain line bounds the region of attraction of the origin.

CLM-P782

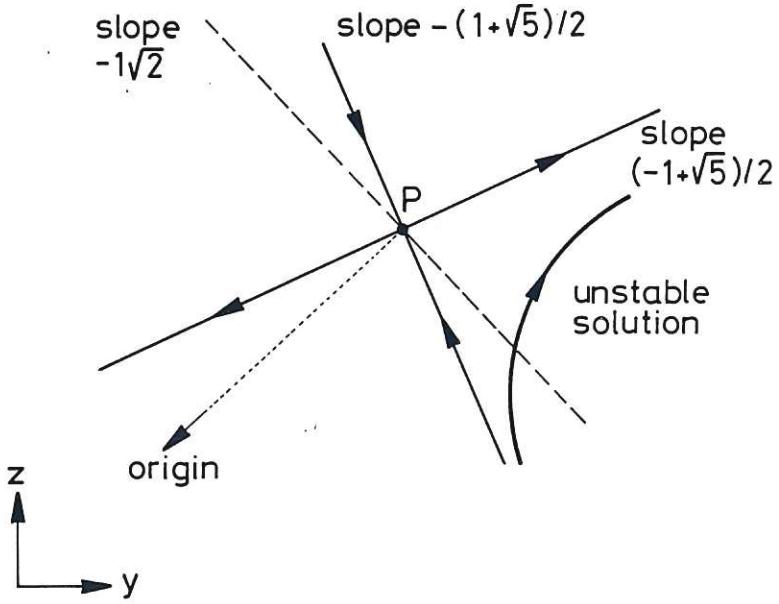

Fig. 3 Separatrices at the unstable fixed point P: $(y, z)=(2\sqrt{2},2)$ for antisymmetric solutions of the non-conservative scheme with $N=4$, coordinates defined by (35). The dashed line is tangent to the circle which corresponds to flows with $Re_m=2\sqrt{3}$.

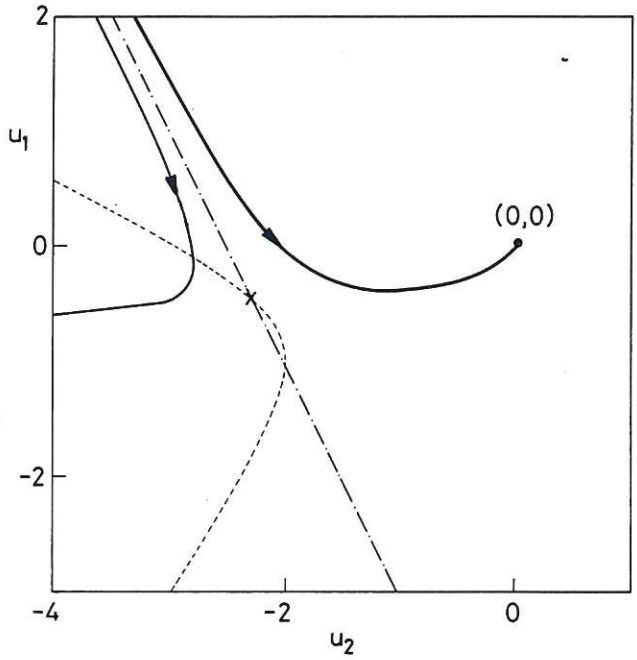

Fig. 4 Phase-plane portrait for antisymmetric solutions of the non-conservative scheme with $N=5$. A second fixed point, $(u_2, u_1)=(\sqrt{5}, -5\ -2\sqrt{5})$ is not shown. Conventions as Fig. 2; the dashed line bounds the region where the total energy always decreases.

CLM-P782

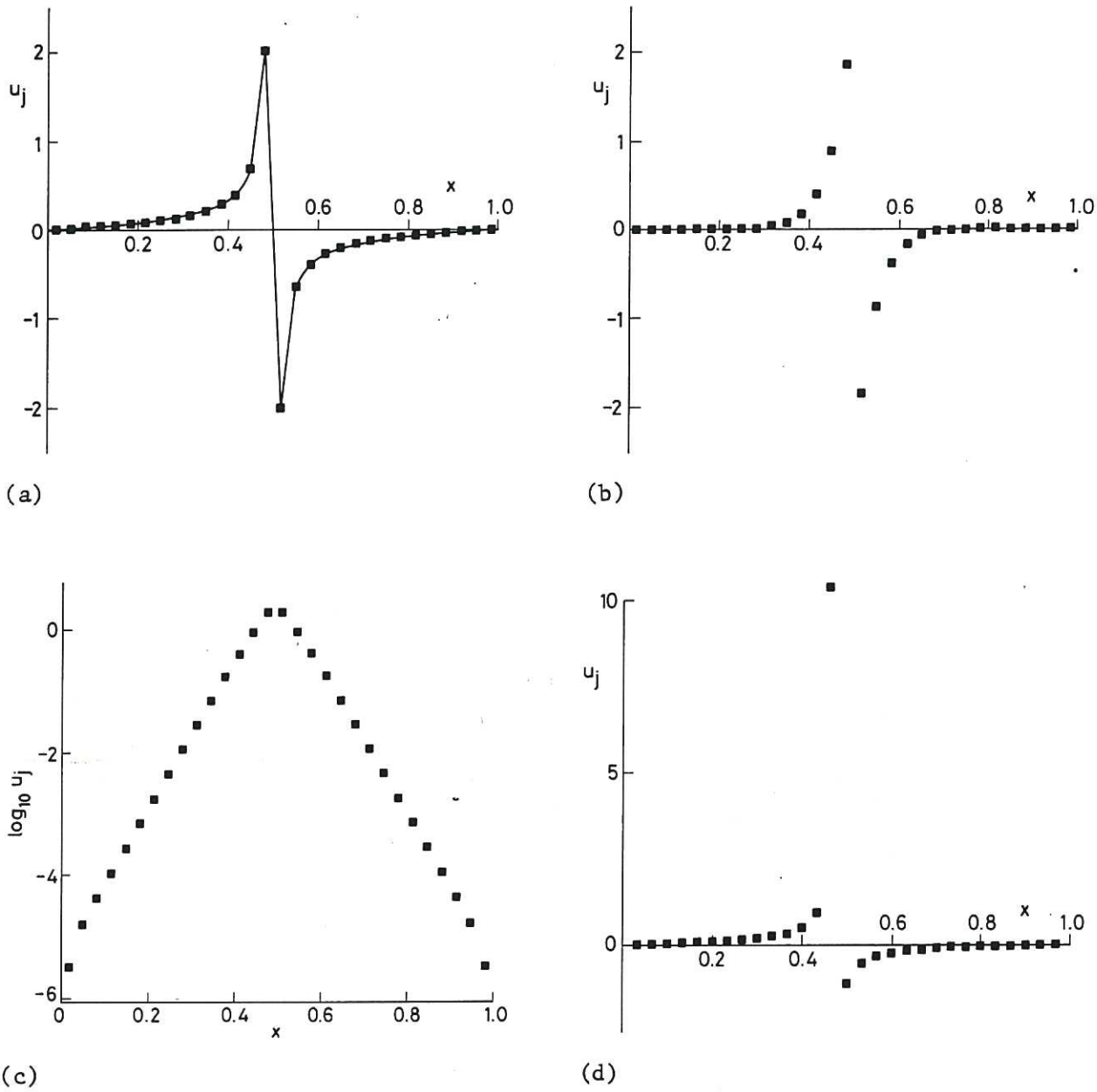

Fig. 5 $\{u_j\}$ plotted as a function of $x=(j+\frac{1}{2})/N$ for the non-conservative difference scheme with $N=30$, (a) corresponding to Re_{mp} when $c=0$, (b) to Re_{mr}, (d) to Re_{mp} when $c=10$. The solid line in (a) joins points $(\pi/N)\tan[\pi(j+\frac{1}{2})/N]$. (c) is (b) replotted on a log scale. N.B. for the unit interval drawn, note that the normalisation reduces u by a factor $0(N)$ relative to that employed in (1b).

CLM-P782